P H Y S I C A L   R E V I E W   L E T T E R S

Near-Field Heat Transfer in a Scanning Thermal Microscope

Achim Kittel, Wolfgang Müller-Hirsch, Jürgen Parisi, Svend-Age Biehs, Daniel Reddig, and Martin Holthaus

Institut für Physik, Carl von Ossietzky Universität, D-26111 Oldenburg, Germany

We present measurements of the near-field heat transfer between the tip of a thermal profiler and planar material surfaces under ultrahigh vacuum conditions. For tip-sample distances below 10^{-8} m, our results differ markedly from the prediction of fluctuating electrodynamics. We argue that these differences are due to the existence of a material-dependent small length scale below which the macroscopic description of the dielectric properties fails, and discuss a heuristic model which yields fair agreement with the available data. These results are of importance for the quantitative interpretation of signals obtained by scanning thermal microscopes capable of detecting local temperature variations on surfaces.

Radiative heat transfer between macroscopic bodies increases strongly when their spacing is made smaller than the dominant wavelength λ_{th} of thermal radiation. This effect, caused by evanescent electromagnetic fields existing close to the surface of the bodies, was already studied theoretically in 1971 by Polder and van Hove for the model of two infinitely extended, planar surfaces separated by a vacuum gap [1], and was reinvestigated later by Loomis and Maris [2] and Volokitin and Persson [3,4]. While early pioneering measurements with flat chromium bodies had to remain restricted to gap widths above 1 μm [5], and later studies employing an indium needle in close proximity to a planar thermocouple remained inconclusive [6], an unambiguous demonstration of near-field heat transfer under ultrahigh vacuum conditions, and thus in the absence of disturbing moisture films covering the surfaces, was given in Ref. [7].

The theoretical treatment of radiative near-field heat transfer is based on fluctuating electrodynamics [8]. Within this framework, the macroscopic Maxwell equations are augmented by fluctuating currents inside each body, constituting stochastic sources of the electric and magnetic fields **E** and **H**. The individual frequency components $\mathbf{j}(\mathbf{r}, \omega)$ of these currents are considered as Gaussian stochastic variables. According to the fluctuation-dissipation theorem, their correlation function reads [9]

$$\langle j_\alpha(\mathbf{r}, \omega) j_\beta^*(\mathbf{r}', \omega') \rangle = \frac{\omega}{\pi} E(\omega, \beta) \epsilon''(\omega) \delta_{\alpha\beta} \delta(\mathbf{r} - \mathbf{r}')$$
$$\times \delta(\omega - \omega'), \quad (1)$$

where $E(\omega, \beta) = \hbar\omega/[\exp(\beta\hbar\omega) - 1]$, with the usual inverse temperature variable $\beta = 1/(k_B T)$; the angular brackets indicate an ensemble average. Moreover, $\epsilon''(\omega)$ denotes the imaginary part of the complex dielectric function $\epsilon(\omega) = \epsilon'(\omega) + i\epsilon''(\omega)$. It describes the dissipative properties of the material under consideration, which is assumed to be homogeneous and nonmagnetic. Thus, Eq. (1) contains the idealization that stochastic sources residing at different points $\mathbf{r}, \mathbf{r}'$ are uncorrelated, no matter

how small their distance may be. Applied to a material occupying the half-space $z < 0$, facing the vacuum in the complementary half-space $z > 0$, these propositions can be evaluated to yield the electromagnetic energy density in the distance z above the surface, giving [10]

$$\langle u(z) \rangle = \frac{\epsilon_0}{2} \langle \mathbf{E}^2 \rangle + \frac{\mu_0}{2} \langle \mathbf{H}^2 \rangle$$
$$= \int_0^\infty d\omega \int_0^\infty d\kappa [\rho_{\mathbf{E}}(\omega, \kappa, \beta, z) + \rho_{\mathbf{H}}(\omega, \kappa, \beta, z)]$$
$$= \int_0^\infty d\omega \frac{E(\omega, \beta)\omega^2}{2\pi^2 c^3}$$
$$\times \left\{ \int_0^1 d\kappa \frac{\kappa}{p} [1 + \kappa^2 \operatorname{Re}(r_\parallel e^{2iz\omega p/c})] \right.$$
$$\left. + \int_1^\infty d\kappa \frac{\kappa^3}{|p|} \operatorname{Im}(r_\parallel) e^{-2z\omega|p|/c} + X_\perp \right\}. \quad (2)$$

Here, the densities $\rho_{\mathbf{E}}$ and $\rho_{\mathbf{H}}$ symbolically specify the electric and magnetic contribution, respectively; $r_\parallel$ denotes the Fresnel amplitude reflection coefficient for TM modes with a wave vector of magnitude $\omega\kappa/c$ parallel to the surface. The symbol $X_\perp$ abbreviates the corresponding terms for TE modes. The wave vector oriented normal to the surface, of magnitude $\omega p/c$, distinguishes propagating modes with real $p = \sqrt{1 - \kappa^2}$ for $\kappa \leq 1$ from evanescent modes with imaginary $p = i\sqrt{\kappa^2 - 1}$ for $\kappa > 1$.

Expression (2) for the energy density, obtained strictly within the framework of macroscopic electrodynamics, diverges for small distances z from the surface; for $z/\lambda_{\mathrm{th}} \ll 1$, one finds the power law $\langle u(z) \rangle \propto z^{-3}$ [8]. Hence, it has been suggested that also the energy dissipated in the tip of a tiny probe close to the surface should scale inversely proportional to the cube of the tip-sample distance [11,12]. However, the entailing divergence clearly is not borne out by the actual physics [13–15]. The divergence may formally be avoided by replacing the upper boundary of integration, $\kappa = \infty$ in Eq. (2), by a finite cutoff κ_c, thereby excluding the problematic large-wave number contributions to the "evanescent" part of the energy den-

sity [4]. It is important to note that the divergence of the energy density (2) close to the material surface reflects a shortcoming of the underlying macroscopic theory: Considering a metal, the dielectric properties of which are largely determined by the conduction electrons, one expects that any contributions from spatial Fourier components shorter than their mean free path are inadequately dealt with [1]. More generally, the spatial deltalike correlation (1) becomes problematic on length scales such that the microscopic properties of the materials start to make themselves felt. These observations, in their turn, imply that experiments on fluctuating electromagnetic fields in the extreme near-field regime, where traditional macroscopic fluctuating electrodynamics can no longer be taken for granted, may yield important information on microscopic material properties.

In this Letter, we report on measurements of the near-field heat transfer between the tip of a scanning thermal microscope and surfaces of gold (Au) or gallium nitride (GaN). We have fabricated a thermosensor, integrated into the tip of a variable-temperature scanning tunneling microscope (VT-STM), which allows us to determine the heat transfer even for tip-sample distances on the order of 1 nm. We argue that our sensor essentially probes the near-field energy density close to the sample, and demonstrate that the experimental data differ markedly from the standard prediction (2) for distances below 10 nm. A simple but physically motivated ansatz for the description of the short-range dielectric material properties then leads to qualitative agreement with the measured data, allowing one to extract material-dependent length scales L below which the macroscopic theory fails.

When assessing the near-field heat flux between two bodies of different temperature, the precise location of their positions of zero separation is of key importance. Since no body has a mathematically flat surface, this is to some extent a matter of definition. We have chosen to record the heat transfer between a cooled sample and the tip of a VT-STM at nearly room temperature, so that zero separation of the two surfaces corresponds to a certain level of electron coupling, i.e., to a certain tunnel current. To exclude any mechanism of heat transfer other than radiation, one has to work under ultrahigh vacuum (UHV) conditions. Otherwise, any surface adsorbate, or surrounding gas, might result in additional contributions to the heat transfer, masking the radiative effect.

The heat flux between the warm tip and the cooled sample is measured through the resulting slight diminution of the temperature of the very tip compared to the rest of the sensor. Since small temperature differences have to be detected over a small sensor, any self-heating has to be carefully avoided. Therefore, we employ a thermocouple integrated into the tip of our VT-STM. As sketched in Fig. 1(a), a thin platinum wire has been melted into a glass micropipette. Subsequently, the part of the wire protruding from the pipette has been electrochemically etched to form a sharp tip [16]. The pipette has then been covered by a

gold film with a thickness of about 25 nm, having electrical contact with the platinum wire only at the very end of the tip. This end thus forms the measuring contact of the resulting coaxial thermocouple, while the reference contact is located in the back at the support of the micropipette, with good thermal coupling to the surrounding which acts as a heat bath.

The support of the micropipette is sitting in the scanner of a commercial VT-STM in an UHV chamber made by Omicron, held by a ring-shaped magnet. In the hole of the magnet a gold-plated, spring-loaded contact pin makes electrical contact with the platinum wire, thus forming the reference contact. The gold film is grounded, whereas the sample is at the tunnel potential, in order to decouple the tunneling signal from the thermoelectric voltage V_{th}. This voltage is first amplified by a Keithley nanovolt preamplifier (model 1801) and then measured by a high resolution multimeter (Keithley model 2001). The temperature of the sample is lowered during the measurements with liquid nitrogen via a coldfinger to 100 K, establishing a temperature difference between the tip and the sample surface of about 200 K.

The Seebeck coefficient $S = V_{th}/\Delta T$ of our sensor, quantifying the ratio of the generated thermoelectric voltage and the temperature difference ΔT between the two contacts of the thermocouple, is determined with a setup consisting of a droplet of oil held by a small heating coil made of tungsten wire. The temperature of the oil is measured by a commercial type-K thermocouple reaching from one side into the droplet, while the sensor enters it from the other side. The oil temperature can be varied by changing the current through the coil. We obtain $S = 8\ \mu V/K$ at room temperature, which is close to the value found in literature [17].

The heat resistance $R_{th} = \Delta T/\Delta P$ of the sensor, relating the heat power ΔP absorbed or emitted by the tip to the resulting temperature difference between the contacts, was determined by placing the tip in the focus of a 1 mW cw laser diode (wavelength 670 nm). The fraction of the light power which did not hit the tip surface was measured by a power meter positioned behind it. The absorbed power was estimated, according to $\Delta P = (P_0 - P)(1 - R)$, from the difference $P_0 - P$ of the power recorded without and with the tip being present, and the reflectivity $R = 0.96$ of its gold surface at 670 nm [18]. The expected linear dependence of the thermovoltage on the absorbed power is well confirmed in Fig. 1(b), showing our results for two different tips. From the slopes 0.18 and 0.43 $\mu V/\mu W$ we obtain heat resistances of 23 and 54 K/mW, respectively. Knowing both a sensor's Seebeck coefficient S and its heat resistance R_{th}, one can deduce the near-field heat flux ΔP between the tip and a closely spaced sample of different temperature from the observed thermovoltage, according to $\Delta P = V_{th}/(SR_{th})$. Measurements of the distance dependence of the heat transfer were performed by retracting the STM tip from the tunnel distance, while the distance itself was determined by means of the piezocoef-
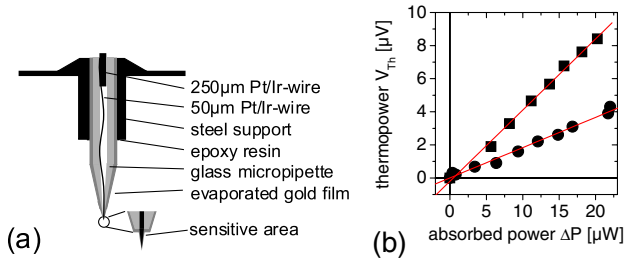
FIG. 1 (color online). (a) Cross section of the micropipette glued into a tip holder. The thermoelectric voltage V_{th} builds up between the inner platinum wire and the outer gold film. The tunnel potential is applied between the sample and the grounded gold film. (b) Dependence of the thermovoltage on the absorbed power ΔP of calibrating laser light for two different sensors.

ficient of the scanner. Results of such measurements are depicted in Fig. 2 for a sample consisting of a gold layer, and in Fig. 3 for a sample of GaN. In both cases, the sensor with $R_{th} = 54$ K/mW has been employed. During these measurements, we have carefully checked that the cross talk between the tunnel current signal and the thermovoltage remains negligibly small. The absence of interference is indicated by the fact that the tunnel current decreases strongly in a range of distances where the observed thermovoltage stays almost constant.

A theoretical discussion of the heat transfer between an idealized tip and a flat surface, which may serve as a guideline for the analysis of our data, has been given by Mulet *et al.* [12]. These authors have modeled the tip by a small dielectric sphere of radius r and assumed the incident electric field to be uniform inside the sphere, so that it acts as a pointlike dipole. If the temperature of the sample is significantly lower than that of the tip, as in our case, the heat current flowing back from the sample to the tip can be
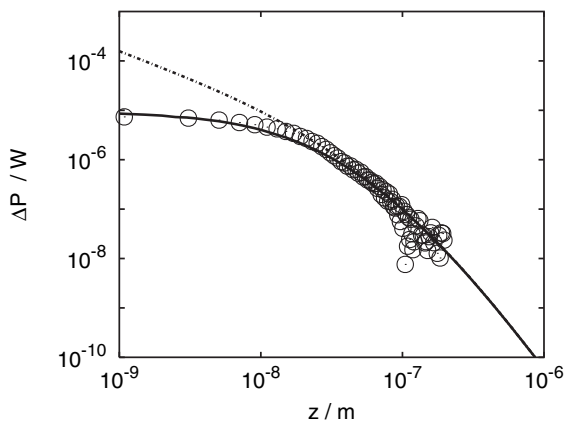
neglected. The total flux between the surface and the tip then is determined entirely by the current directed from the tip to the sample, according to

$$\Delta P = \int_0^\infty d\omega \int_0^\infty d\kappa\, \alpha(\omega) \rho_E(\omega, \kappa, \beta, z), \qquad (3)$$

where $\alpha(\omega) = 2\omega(4\pi r^3)\epsilon''_{tip}/|\epsilon_{tip} + 2|^2$ describes the dielectric properties of the sphere, and the temperature entering ρ_E is that of the tip. Taking this expression at a representative frequency ω_0, one has $\Delta P \approx \alpha(\omega_0)\epsilon_0\langle E^2\rangle/2$, so that, within the scope of the model, the heat flux registered by the tip should be proportional to the electrical energy density of the flat sample, evaluated, however, at the temperature of the tip.

For distances larger than about 10^{-8} m, our experimentally observed heat transfer is, to good accuracy, proportional to the *total* energy density as given by Eq. (2), not to the electric field contribution alone. Since the constant of proportionality, which carries the dimension of area times velocity, may differ substantially from $\alpha(\omega_0)$, we focus on the scaled energy density $\Delta P_{th} := \pi a^2 c \langle u(z)\rangle$, where c is the velocity of light, and employ the effective sensor area πa^2 as a fitting parameter. Modeling the dielectric function $\epsilon(\omega)$ for Au by a Drude ansatz with parameters taken from Ref. [19], and that for GaN by the "reststrahlen" formula with parameters from Ref. [20], we obtain the dashed lines in Figs. 2 and 3, setting $a = 60$ nm. This value is in accordance with scanning electron microscopy studies of the tip and describes *both* experimental data sets for $z \gtrsim 10$ nm, as it should. The latter fact also indicates that the use of Eq. (2), i.e., the neglect of the field's distortion by the tip, is justified here.

In the case of GaN, the theoretical curve for ΔP_{th} diverges as z^{-3} for sensor-sample distances below 10 nm. In contrast, for Au this familiar behavior would become apparent only at substantially smaller z [3]. However, the experimental data clearly show a different trend, leveling off to values which for the smallest accessible distances are significantly lower than ΔP_{th}. We interpret this finding as
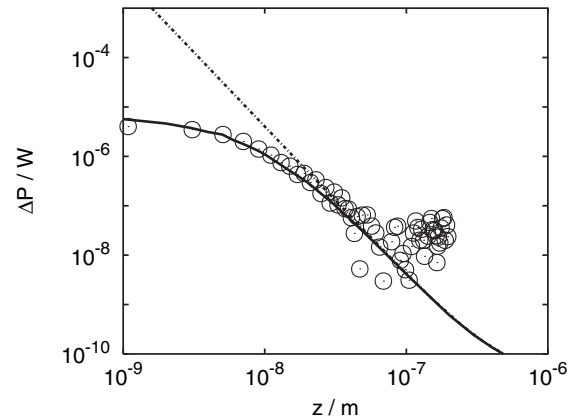

FIG. 2. Measured heat current ΔP (in Watts) between the microscope tip and a gold layer (circles) vs tip-sample distance z. The dashed line, which coincides with the solid one for larger z, corresponds to the prediction ΔP_{th} of standard fluctuating electrodynamics, based on Eq. (2). The solid line is obtained from Eq. (5) with the modified dielectric function (4), setting $L = L_{tip} = 1.2 \times 10^{-8}$ m.

FIG. 3. As Fig. 2 for a sample of GaN, setting $L = 1.0 \times 10^{-10}$ m and $L_{tip} = 1.2 \times 10^{-8}$ m.

evidence for the short-distance deficiency of the macroscopic theory, as expressed by the deltalike correlation function (1) of the stochastic source currents: In a real sample, there is some finite correlation length L.

In principle, one should then also account for nonlocal effects, which requires distinguishing a transversal and a longitudinal part of the permittivity [21]. We do not resort to the systematic theory of such effects here, but propose a qualitative approach: Since it appears necessary to smooth out the correlation function (1) on short distances, one might introduce an appropriate modification of the imaginary part of $\epsilon(\omega)$. However, then the Kramers-Kronig relation requires a corresponding modification of the real part. Hence, a heuristically motivated, plausible ansatz for an effective permittivity depending explicitly on the transversal wave number is

$$\tilde{\epsilon}(\omega, \kappa) := 1 + [\epsilon'(\omega) - 1]f(\kappa) + i\epsilon''(\omega)f(\kappa), \quad (4)$$

where the function $f(\kappa)$ accounts for the lateral correlations, such that it approaches unity and thereby restores the local case when $\omega\kappa/c \ll L^{-1}$, but vanishes for large-wave numbers, when $\omega\kappa/c \gg L^{-1}$. As a convenient guess, we take a Gaussian $f(\kappa) = \exp[-(L\omega\kappa/c)^2]$ and consider L as a parameter to be determined by fitting the data. When evaluating the Maxwell equations for systems with plane translational invariance [1], we replace $\epsilon(\omega)$ by $\tilde{\epsilon}(\omega, \kappa)$. The energy density can then again be obtained from Eq. (2), if the reflection coefficients $r_\parallel$ and $r_\perp$ are adapted in this manner.

Besides the dielectric properties of the sample, also those of the sensor enter into the data, as exemplified by the dipole model (3). Hence, we have to introduce both a correlation length L of the sample and a further correlation length L_{tip} of the sensor, and parametrize the experimentally observed heat current in the form

$$\frac{\widetilde{\Delta P}}{\pi a^2 c} = \int_0^\infty d\omega \int_0^\infty d\kappa \, e^{-(L_{tip}\omega\kappa/c)^2}$$
$$\times [\rho_\mathbf{E}(\omega, \kappa) + \rho_\mathbf{H}(\omega, \kappa)]. \quad (5)$$

Using this ansatz (5), we finally obtain the solid curves in Figs. 2 and 3, setting $L = 1.2 \times 10^{-8}$ m for Au and $L = 1.0 \times 10^{-10}$ m for GaN, while $L_{tip} = 1.2 \times 10^{-8}$ m in both cases. These curves capture the experimental data quite well, thus lending strong support to our line of reasoning. It is also encouraging to observe that the numerical value of L obtained for Au indeed turns out to be on the order of the mean free path of electrons in metals, whereas that for GaN is considerably shorter, as it should. Although the thermally relevant component of our sensor probably is confined to the Au layer, its correlation length does not necessarily have to coincide with that of the gold sample, as it actually does in our case, but might be geometrically restricted in alternative setups.

In summary, we have obtained experimental data for the near-field heat transfer between a thermal profiler and flat material surfaces under UHV conditions. We have reached the extreme near-field regime, where the variation of the heat transfer rate with the distance between microscope tip and sample differs distinctly from the divergent behavior predicted by standard macroscopic fluctuating electrodynamics, and have interpreted our observations in terms of finite microscopic correlations inside the materials. While the shortcomings of the macroscopic theory are, in principle, well known [8,9], their manifestation in an actual experiment indicates a still unexplored potential of thermal microscopy as a new, quantitative tool for the nanometer-scale investigation of solids.

[1] D. Polder and M. van Hove, Phys. Rev. B **4**, 3303 (1971).
[2] J. J. Loomis and H. J. Maris, Phys. Rev. B **50**, 18 517 (1994).
[3] A. I. Volokitin and B. N. J. Persson, Phys. Rev. B **63**, 205404 (2001).
[4] A. I. Volokitin and B. N. J. Persson, Phys. Rev. B **69**, 045417 (2004).
[5] C. M. Hargreaves, Phys. Lett. **30A**, 491 (1969).
[6] J.-B. Xu, K. Läuger, R. Möller, K. Dransfeld, and I. H. Wilson, J. Appl. Phys. **76**, 7209 (1994).
[7] W. Müller-Hirsch, A. Kraft, M. Hirsch, J. Parisi, and A. Kittel, J. Vac. Sci. Technol. A **17**, 1205 (1999).
[8] S. M. Rytov, Yu. A. Kravtsov, and V. I. Tatarskii, *Principles of Statistical Radiophysics* (Springer, New York, 1989), Vol. 3.
[9] E. M. Lifshitz and L. P. Pitaevskii, *Statistical Physics*, Landau-Lifshitz, Course of Theoretical Physics Vol. 9, Pt. 2 (Butterworth-Heinemann, Oxford, 2002).
[10] K. Joulain, R. Carminati, J.-P. Mulet, and J.-J. Greffet, Phys. Rev. B **68**, 245405 (2003).
[11] I. A. Dorofeyev, J. Phys. D **31**, 600 (1998).
[12] J.-P. Mulet, K. Joulain, R. Carminati, and J.-J. Greffet, Appl. Phys. Lett. **78**, 2931 (2001).
[13] J. L. Pan, Opt. Lett. **25**, 369 (2000).
[14] J.-P. Mulet, K. Joulain, R. Carminati, and J.-J. Greffet, Opt. Lett. **26**, 480 (2001).
[15] J. L. Pan, Opt. Lett. **26**, 482 (2001).
[16] L. Libioulle, Y. Houbion, and J. M. Gilles, Rev. Sci. Instrum. **66**, 97 (1995).
[17] M. Gotoh, K. D. Hill, and E. G. Murdock, Rev. Sci. Instrum. **62**, 2778 (1991).
[18] J. Bass, J. Dugdale, C. Foiles, and A. Myers, in *Electrical Resistivity, Thermoelectrical Power and Optical Properties*, Landolt-Bornstein, Metals: Electronic Transport Phenomena, Group III, Vol. 15, Pt. b (Springer, Berlin, 1985).
[19] N. W. Ashcroft and N. D. Mermin, *Solid State Physics* (Harcourt, Fort Worth, 1976).
[20] S. Adachi, *Handbook on Physical Properties of Semiconductors* (Kluwer, Boston, 2004).
[21] V. Ginzburg, *Applications of Electrodynamics in Theoretical Physics and Astrophysics* (Gordon and Breach, New York, 1989).